Computer simulation of a two-dimensional type-II superconductor in a magnetic field

1991 J. Phys.: Condens. Matter 3 375

(http://iopscience.iop.org/0953-8984/3/3/013)

J. Phys.: Condens. Matter 3 (1991) 375–380. Printed in the UK

LETTER TO THE EDITOR

Computer simulation of a two-dimensional type-II superconductor in a magnetic field

Yoshihisa Enomoto† and Ryuzo Kato‡

† Department of Physics, Faculty of Science, Nagoya University, Nagoya 464-01, Japan

‡ Department of Applied Physics, Faculty of Engineering, Nagoya University, Nagoya 464-01, Japan

Received 12 November 1990

Abstract. We study the time-dependent behaviour of type-II superconductors in an external magnetic field. Based on the time-dependent Ginzburg–Landau equation, simulations for several situations are performed in two dimensions in order that we might discuss the dynamical behaviour of magnetic flux structures.

With the discovery of high-T_c superconductors, solving the Ginzburg–Landau (GL) equation has recently attacted much attention in the discussion of magnetic flux structures [1]. Several computational attempts at a solution have been made [2–5]. However, none of the previous authors has directly dealt with the time-dependent Ginzburg–Landau (TDGL) equations in the presence of an external magnetic field. Thus our primary concern here is a visualization of the dynamical behaviour of type-II superconductors, based on the TDGL equations.

The dynamics of superconductors is phenomenologically described by the following TDGL equations [6]:

$$D^{-1}\left(\frac{\partial}{\partial t}+\mathrm{i}\frac{2e\psi}{\hbar}\right)\Delta+\xi^{-2}(|\Delta|^2-1)\Delta+\left(\frac{\nabla}{\mathrm{i}}-\frac{2e}{\hbar c}A\right)^2\Delta=0 \tag{1}$$

$$j=\sigma\left(-\nabla\psi-\frac{1}{c}\frac{\partial A}{\partial t}\right)+\mathrm{Re}\left[\Delta^*\left(\frac{\nabla}{\mathrm{i}}-\frac{2e}{\hbar c}A\right)\Delta\right]\frac{\hbar c^2}{8\pi e\lambda^2} \tag{2}$$

where Δ, A, ψ and j are the complex order parameter, vector potential, scalar potential and current density, respectively. Here D and σ are the normal state diffusion constant and conductivity, respectively. The temperature-dependent coherence length is ξ and the temperature-dependent magnetic penetration depth is λ. In the case where electric effects, such as transport current, are neglected, the following equations are added to the above [6]:

$$j=(c/4\pi)\nabla\times\nabla\times A \tag{3}$$

$$E=-(1/c)\,\partial A/\partial t-\nabla\psi \tag{4}$$

0953-8984/91/030375 + 06 $03.50

$$\boldsymbol{B} = \nabla \times \boldsymbol{A} \tag{5}$$

It should be pointed out that a gauge transformation of the potentials

$$\boldsymbol{A} \rightarrow \boldsymbol{A} - \nabla\chi \qquad \psi \rightarrow \psi + (1/c)\,\partial\chi/\partial t \tag{6}$$

accompanied by a phase definition of Δ,

$$\Delta \rightarrow \Delta \exp\left(-\mathrm{i}\frac{2e}{\hbar c}\chi\right) \tag{7}$$

leaves equations (1)–(5) unchanged. This means that the physical results are independent of the choice of χ. Thus, in order to make the scalar potential zero, we set $\partial\chi/\partial t = -c\psi$.

These equations can be rescaled to measure

$$r \text{ in units of } l \equiv \xi/a \tag{8}$$

$$t \text{ in units of } t_{\mathrm{GL}}/12 \tag{9}$$

$$\boldsymbol{A} \text{ in units of } \sqrt{2}H_{\mathrm{c}}\kappa l \tag{10}$$

$$\psi \text{ in units of } \hbar/2et_{\mathrm{GL}} \tag{11}$$

with

$$t_{\mathrm{GL}} \equiv \pi\hbar/8k_{\mathrm{B}}(T_{\mathrm{c}} - T) \tag{12}$$

$$\kappa \equiv \lambda/\xi \tag{13}$$

where a in equation (8) is a positive constant and is determined later so as to make the numerical calculation efficient, H_{c} is the critical magnetic field, and T_{c} the critical temperature. Then, in normalized dimensionless units the above equations of motion can be rewritten as

$$\partial\Delta/\partial t = -(1/12)[(a\nabla/\mathrm{i} - \boldsymbol{A}/a)^2\Delta + (|\Delta|^2 - 1)\Delta] \tag{14}$$

$$\partial\boldsymbol{A}/\partial t = (a^2/2\mathrm{i})(\Delta^*\nabla\Delta - \Delta\nabla\Delta^*) - |\Delta|^2\boldsymbol{A} - \kappa^2a^2\nabla \times \nabla \times \boldsymbol{A}. \tag{15}$$

In the following discussion we consider a flat square plate of type-II superconductor ($\kappa > 1/\sqrt{2}$) in the x–y plane with a magnetic field incident in the z-direction. We also assume that the plate is surrounded by the insulator. We are interested in field configurations invariant under a translation along the z-axis. Thus, all the fields depend only on the x- and y-coordinates, and the third components of the fields are neglected.

Now we carry out two-dimensional computer simulations of the TDGL equations on an N^2 square lattice. In our simulations we use the simple Euler method with the time step $\Delta t = 0.05$, the space step $\Delta x = \Delta y = 1$, and $a = 2$. The grid size is 60×60 ($N = 60$) and thus the space size is $30\xi \times 30\xi$ in physical units. We also set $\kappa = 2$. Note that in these normalized units the upper critical field $H_{\mathrm{c2}} = 1$ and the lower critical field $H_{\mathrm{c1}} \approx \ln\kappa/2\kappa^2 = 0.087$.

The boundary conditions (BC) are assumed to be as follows;

$$(a\nabla/\mathrm{i} - \boldsymbol{A}/a)\,\Delta|_{\mathrm{n}} = 0 \tag{16}$$

$$\nabla \times \boldsymbol{A} = \boldsymbol{H}_{\mathrm{e}} \tag{17}$$

where the index n in equation (16) denotes the normal direction on the boundary. The BC (16) means that the system considered here is surrounded by the insulator, while the BC (17) means that the vector potential on the boundary is determined by the external

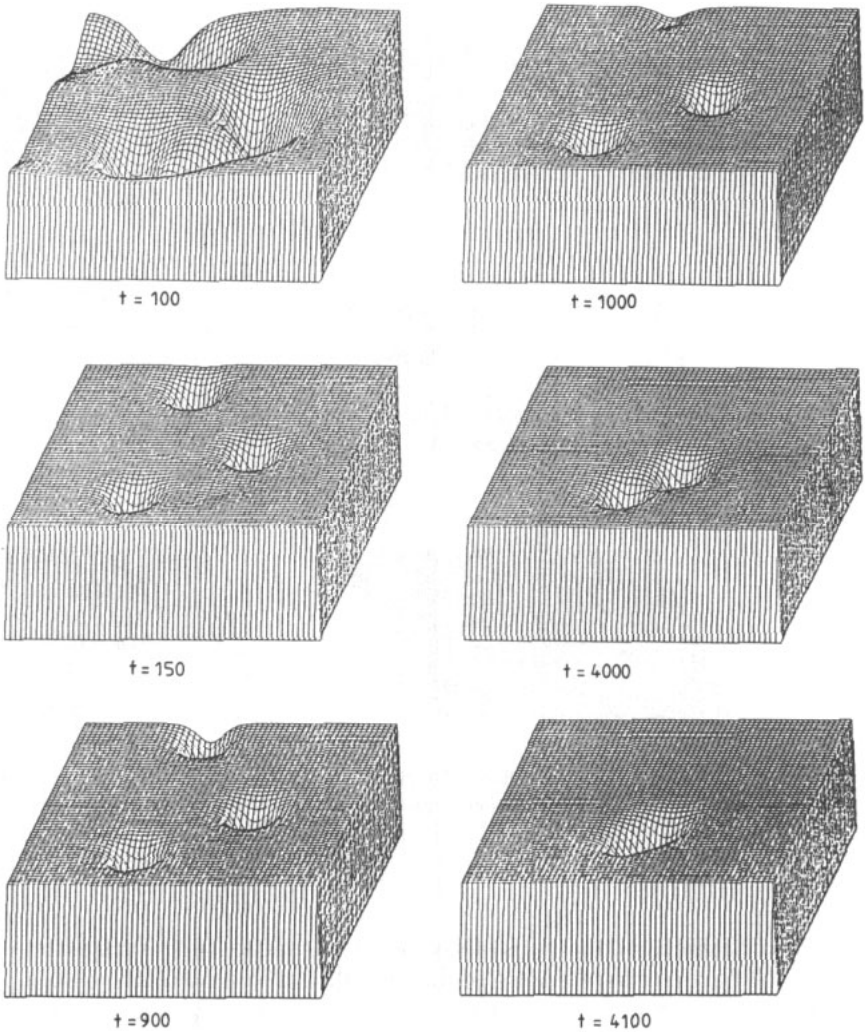

Figure 1. Time evolutions of the spatial pattern of $|\Delta|$ for $h_e = 0$. The profiles of the magnitude of $|\Delta|$ are shown at various times. The maximum value is 1.0 and the minimum value is 0.01 in this time series.

magnetic field $\boldsymbol{H}_e = h_e(x, y)\hat{z}$, where $\hat{z}$ is the unit vector along the z-axis. Initially at each lattice site both real and imaginary parts of Δ are chosen to be parts of a Gaussian random number with average 0 and variance 0.01, while we set $A = (A_x, A_y) = (0, 0)$.

Before studying the complicated situation, we numerically check the range of validity of our simulation using the two analytic stationary solutions of the TDGL equations. One is a one-vortex solution at $h_e = H_{c1}$ [6], and the other is a well-known Abrikosov flux lattice solution at $h_e \lesssim H_{c2}$ [7]. We have numerically found that the one-vortex solution is stable, while the Abrikosov solution is unfortunately unstable or destroyed in our simulation. Taking into account the Abrikosov assumption of an infinite system, the finiteness of the present simulation is thought to cause this undesirable situation. In order to avoid this, we need to simulate a fairly large system using a more complicated

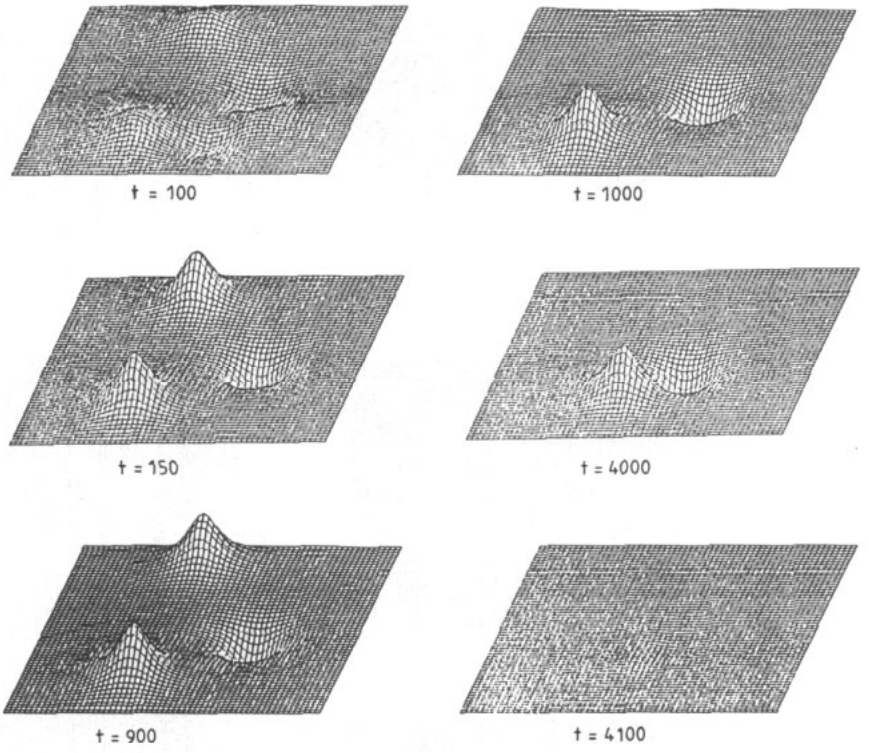

Figure 2. Time evolutions of spatial pattern of B_z for $h_e = 0$. The profiles of the magnitude of B_z are shown at various times. The maximum value is 0.23 and the minimum value is −0.23 in this time series.

difference scheme and methods of saving computational time, such as an introduction of thermal fluctuations. Because of the limitation of our computer system, and as the first step of our work, we carry on in the present manner which is thought to be valid at least for $h_e \ll H_{c2}$.

At first we study a case for $h_e = 0$. In this case a configuration with $|\Delta| = 1$ and no magnetic field is known to be stable. In figures 1 and 2 the time developments of the patterns of Δ and B_z are shown, respectively, where B_z is defined by $B_z \equiv \partial A_x/\partial y - \partial A_y/\partial x$. As is expected, the system asymptotically approaches the global uniform state. Note that in this case localized magnetic field configurations exist in the system. Hereafter a localized magnetic configuration with B_z along the positive (negative) z-direction is called an (anti-) vortex. Typical patterns of current density j near vortices are shown in figure 3. Note that we have numerically checked that each vortex configuration is quantized and thus that its magnetic flux is equal to the elementary flux quantum, $\Phi_0 \equiv hc/2e$. From these figures we find that the removal of a vortex from the edge and a pair annihilation of a vortex and anti-vortex take the system to the uniform state. This result for the case without the external field is similar to that of a previous simulation where the vector potential A was completely neglected [8].

Next, we study a case for $h_e = 0.2$. In this case, $H_{c1} < h_e < H_{c2}$, no detailed analytic discussion exists. However, it is expected from analogy with the Abrikosov discussion that a state with a regular vortex lattice is stable. In figure 4 we can see that initially

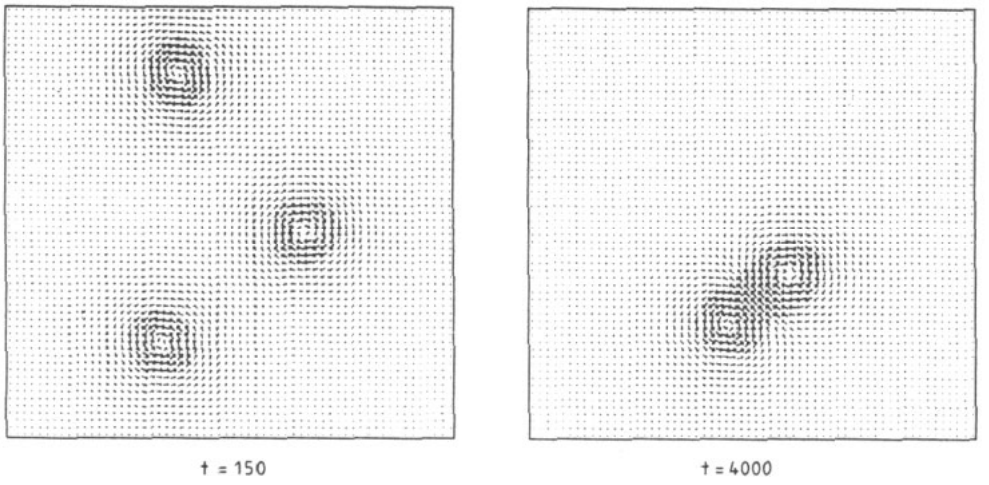

Figure 3. Spatial patterns of j for $h_e = 0$ at $t = 150$ and 4000. The direction of an arrow denotes the direction of a current flow. Moreover, each arrow's size and shade correspond to the amplitude of current. The maximum value is 0.05 and the minimum value is 0 in this time series.

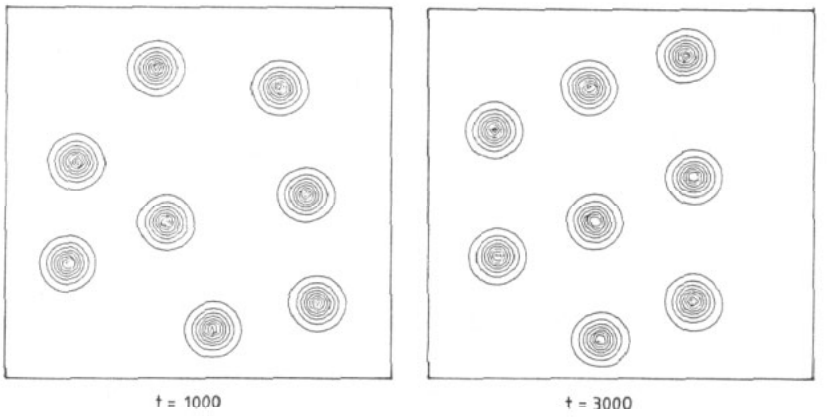

Figure 4. Time evolutions of the spatial pattern of $|\Delta|$ for $h_e = 0.2$. The contour lines of $|\Delta$ with interval 0.1 are shown at $t = 1000$ and 3000.

random positions of vortices tend to become regular. We have numerically checked that the pattern at $t = 3000$ is rarely changed even after long time calculations. As far as we know, this is the first simulation to have visualized the time-dependent behaviour of a vortex lattice regularization.

Finally we study the effects of impurities on the vortex motion. Here we simply represent an impurity at position (x_0, y_0) such that at this position the value of $|\Delta(x_0, y_0)|$ is forced to be zero. In the following, the analytic one-vortex solution is chosen as the initial state, and a position (20, 30) is set as its starting position. In figure 5 we show the trajectories of a vortex for various positions of one impurity with $h_e = 0$. If there is

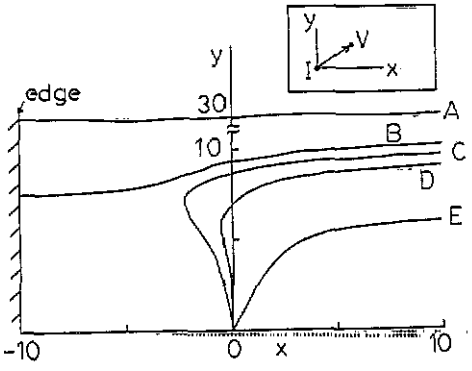

Figure 5. Trajectories of a vortex according to various impurity positions with $h_e = 0$. These trajectories are seen from the impurity position, as shown in the inset, where the symbol 'V' denotes the vortex and 'I' the impurity. The trajectories C–E end in pinnings.

no impurity, the vortex is removed away from the system, because $h_e = 0$. This case is shown in figure 5 by trajectory A. We find the existence of a pinning threshold between trajectories B and C.

In summary we have caried out several simulations of the TDGL equations and reproduced the typical pattern evolutions of Δ and B_z. We have found that the present direction of research may provide us with a useful tool in studying the time-dependent behaviour of superconductors. Studying the effects of random impurities, transport current and thermal fluctuations, as well as the intermediate state in type-I superconductors, is interesting and they still remain open problems. These problems could be discussed within the present framework [9]. We also expect that an essence of the time-dependent behaviour of the magnetic flux structures in high-T_c superconductors can be caught through the present simulation.

The authors are grateful to Professor S Maekawa for a number of valuable discussions.

References

[1] For a review, see
Ginsberg D M (ed) 1989 *Physical Properties of High Temperature Superconductors* (Singapore: World Scientific)
See also
Bednorz J F *et al* (ed) 1990 *Earlier and Recent Aspects of Superconductivity* (Berlin: Springer)
[2] Jacobs L and Rebbi C 1979 *Phys. Rev.* B **19** 4486
[3] Yang Y 1990 *J. Math. Phys.* **31** 1284
[4] Doria M M, Guvernatis J E and Rainer D 1990 *Phys. Rev.* B **41** 6335
[5] Garner J and Benedek R 1990 *Phys. Rev.* B **42** 6027
[6] Tinkham M 1975 *Introduction to Superconductivity* (New York: McGraw-Hill)
[7] Abrikosov A A 1957 *Sov. Phys.–JETP* **5** 1174
[8] Enomoto Y and Kato R 1989 *Phys. Lett.* A **142** 256
[9] Kato R, Enomoto Y and Maekawa S 1990 in preparation